Design and Evaluation of an Active Ripple Filter with Rogowski-Coil Current Sensing

Mingjuan Zhu David J. Perreault Vahe Caliskan
Timothy C. Neugebauer Stephan Guttowski John G. Kassakian

Massachusetts Institute of Technology
Laboratory for Electromagnetic and Electronic Systems
Cambridge, MA 02139 USA

Abstract - An active ripple filter is an electronic circuit which cancels or suppresses the ripple current and EMI generated by the power stage of a power converter, thus reducing the passive filtration requirements. This paper presents the design and evaluation of a feedforward active ripple filter which employs a Rogowski coil for ripple current sensing. The design of the active filter is discussed in detail, including the advantages, tradeoffs, and limitations of the approach. Experimental results from a prototype converter system using this approach are presented, and quantitative comparisons are made between a hybrid passive/active filter and a purely passive filter. It is demonstrated that substantial improvements in filter mass and converter transient performance can be achieved using the proposed active ripple filtering method.

I. INTRODUCTION

Input and output filters have become an extremely important part of modern switching power converters, and often account for a substantial portion of converter size and cost. Traditionally, passive LC low-pass filters have been employed to attenuate power converter switching ripple to acceptable levels [1,2]. However, the tight ripple specifications that are often imposed for application reasons or to meet conducted EMI specifications can result in bulky and expensive filters which are detrimental to the transient performance of the system. This is especially true for systems which operate at low voltage and/or high current levels, due to the nature of the filter components and their parasitics.

An alternative to the conventional approach is the use of an active ripple filter, in which an active electronic circuit (typically coupled with a reduced passive filter) is used to cancel or suppress ripple components at the filter output [3-9]. Typically, the reduced passive filter attenuates the ripple to an intermediate level at which the active electronics can cancel or suppress the ripple to an even lower level without undue power loss. For example, Fig. 1 shows a feedforward active ripple filter used in conjunction with a passive filter at the output of a buck converter. The active filter senses the ripple current in the passive filter inductance and shunts an exact copy of it away from the output capacitance and load. This reduces the ripple seen at the output, and permits a substantially smaller passive filter to be employed than would otherwise be possible. Potential benefits of the active filter approach thus include reduction of the converter size and cost, and improvements in transient performance.

Many types of active ripple filters are possible. Ripple-current filters (such as the one illustrated in Fig. 1) reduce the ripple current passing through a circuit branch [4-9], while ripple-voltage filters reduce the voltage ripple at a node [3,4]. Feedforward filters achieve the ripple reduction by measuring a ripple component and injecting its inverse [6-8], while feedback filters operate to suppress the ripple via high-gain feedback control [3-5,7,9]. Hybrids of these filter types are also possible (see [7], for example), and active filters may be further classified by how the sensing and driving functions are implemented [4].

This paper presents the design and evaluation of a feedforward ripple-current active filter which employs a Rogowski coil for ripple current sensing. While the Rogowski coil sensing technique has not been previously employed for active ripple filters, it is advantageous in this application due to its high accuracy and bandwidth, low weight and cost, and low sensitivity to parameter variations. Section II of the paper describes the design of the active filter elements, including the Rogowski-coil sensor and amplifier electronics, and the class A current injector circuit. Application of the active filter technique to the output filter of a prototype power converter is described in Section III. The active filter elements are coupled with a small passive filter to form a hybrid passive/active output filter. Section IV of the paper presents experimental results from the prototype converter system, and compares the hybrid passive/active filter to an entirely passive filter which meets the same ripple attenuation specification. Finally,

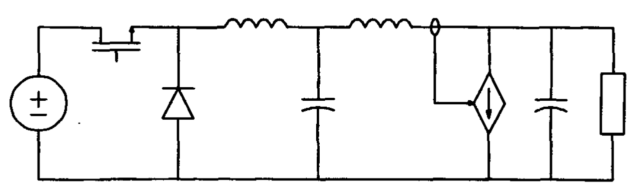

Figure 1 A feedforward current-ripple active filter used in conjunction with a passive filter on the output of a buck converter. The active filter allows a much smaller passive filter to be employed.

Section VI draws conclusions and presents an evaluation of the new active filtering approach.

II. The Active Filter

Successful implementation of a feedforward current-ripple cancellation scheme (such as illustrated in Fig. 1) requires that the ripple current be both sensed and replicated with great fidelity. Therefore, the current sensor and injector must each have wide bandwidth, an accurately known gain with low sensitivity to parameter variations, and low phase distortion.

A. Current Sensing

One approach that has been used to sense ripple current for active filtering is integrating the voltage across a converter or filter inductor, either directly or through the use of a second sense winding [6,8]. While the approach is very inexpensive, it is also problematic because the sensor gain depends directly on inductance (which can vary across different units, time, temperature, and flux levels), though these limitations can be partially mitigated through the use of adaptive tuning methods [6]. Current transformers have also been employed for current ripple sensing in active filters [7,9]. While this approach can yield isolated, high bandwidth measurements, the current transformer must be designed so that it does not saturate while carrying the dc component of the primary current, which increases its size and cost.

B. Rogowski Coil Sensor

In the active filter described here, we have implemented a current ripple sensor based on a Rogowski coil [10-12]. The Rogowski sensing technique has been known since 1912 [10], but has typically been used to sense large currents [11,12] because of the low gain of the coil. In the system described here, the sensed ripple current levels are only on the order of 100 mA, but we have been able to adapt it for these levels through proper amplifier design.

The Rogowski coil itself comprises a uniform single-layer winding on a nonmagnetic toroidal core (Fig. 2). The open-circuit voltage induced on the winding is proportional to the derivative of the current passing through the toroid:

$$v = \frac{\mu_0 N A_t}{l_c} \frac{di}{dt} = k \frac{di}{dt} \tag{1}$$

where N is the number of winding turns, A_t the cross-sectional area of the toroid, and l_c is the mean path length around the toroid. An integrating amplifier stage is then used to convert this signal into an output voltage that is proportional to the input current waveform. This sensing technique has a number of advantages which make it well-suited to this application: it is accurate and has very high bandwidth, yields an isolated output signal and does not load the circuit, it is insensitive to system parameter variations and does not suffer from dc-current saturation effects, and is relatively simple and inexpensive to manufacture.

The design of the coil is governed by a number of factors. Given a maximum practical ratio of the toroid cross section to circumference (A_t / l_c), the only methods to increase the gain of the coil are to increase its size (both A_t and l_c in proportion), or to increase the number of turns on the coil, or to increase the number of times the current to be sensed is passed through the toroid. The size of the coil and the number of times the current to be sensed is passed through it are limited by the desire to have a compact, inexpensive sensor. Increasing the number of turns on the coil increases the output inductance of the coil, which limits the high-frequency performance of the sensor. To understand this, consider that a basic Thévenin model for the coil is the induced voltage (from the sensed current) in series with the coil inductance. To keep the high-frequency impedance at the coil output node low (for converter noise rejection) and to prevent the coil inductance from resonating with the amplifier input, the coil needs to be terminated with a sufficiently low resistance (typically in the kΩ range) by the amplifier. The output inductance of the coil forms a low-pass filter with the amplifier input impedance, affecting the phase (and eventually the magnitude) of the amplified signal. Thus, to achieve good high-frequency performance, there is a limit on the acceptable coil output inductance, and hence on the number of coil turns used.

In the prototype Rogowski coil, these factors were traded off against one another, resulting in good sensing gain and bandwidth for ripple currents at the 100 mA level in the 100+ kHz range. The toroid (i.d. = 18 mm , o.d. = 32 mm, height = 13 mm), was wound with 88 turns of 31 gage wire, and the current to be sensed was passed through the coil 5 times, yielding a total gain k of 6.4×10^{-7} V-s/A. The 14 μH output inductance of the coil was terminated with an amplifier input resistance of 1 kΩ, yielding acceptable bandwidth and damping.

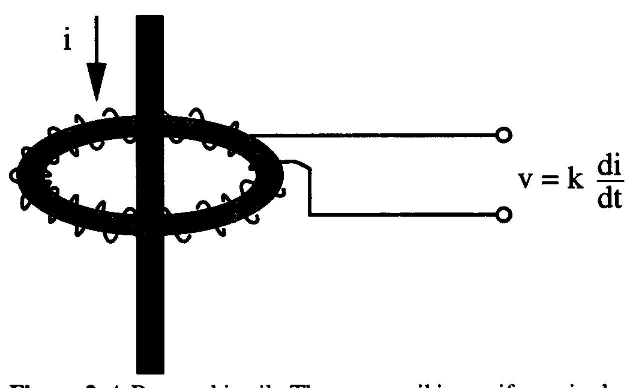

Figure 2 A Rogowski coil. The sense coil is a uniform single-layer winding on an air-core former.

C. Amplifier Electronics

To adapt the Rogowski sensing technique to the low ripple current levels encountered in active filtering applications, a

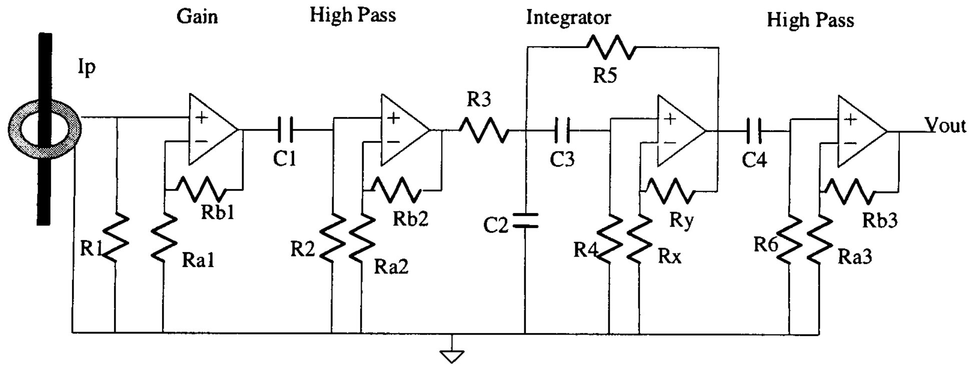

Figure 3 Amplifier for the Rogowski-coil current sensor. The circuit is based on an LT1230 quad current-feedback amplifier. $R_{a1} = R_{a2} = R_{a3} = 220\ \Omega$, $R_{b1} = R_{b2} = R_{b3} = 820\ \Omega$, $R_1 = R_2 = R_6 = 1\ k\Omega$, $R_3 = R_4 = 750\ \Omega$, $R_5 = 4.3\ k\Omega$, $R_x = 200\ \Omega$, $R_y = 4.2\ k\Omega$.

four-stage amplifier based on a single LT1230 quad current-feedback op amp IC was developed (Fig. 3). The amplifier performs the necessary frequency shaping and amplification for ripple-frequency components, while rejecting low-frequency components. The amplifier is composed of four stages: a gain stage and two high-pass/gain stages, each with a pass-band gain of 4.7, and a ripple-frequency integrator stage. The integrator stage acts as a differentiator (gain increasing 20 dB/decade) for frequencies below 1 kHz, and acts as an integrator (gain decreasing 20 dB/decade) for higher frequencies (with a gain of 0.16 at 100 kHz). To meet the high-gain, high-bandwidth requirements of the system with small phase shift at the frequencies of interest, current feedback op amps are used. The op amps are configured as noninverting (fixed gain) amplifiers, and are used along with passive elements to achieve the necessary filtering and amplification. With this four-stage amplifier, the current sensor has a mid-band gain of 6.6 V/A, and a useful bandwidth of approximately 1 MHz.

D. Current Injector

The second major active filter element is the current injector. The current injector is designed to inject an exact replica of the sensed current (with opposite polarity) at the output of the active filter, thus canceling the sensed ripple current. As with the current sensor, it must have high accuracy, wide bandwidth, and a small phase shift in order to be effective. To achieve the required performance, the current injector is typically implemented with linear amplifier circuits, making it a dissipative element. Nevertheless, it should be pointed out that while the injected ripple currents may be large, the power injected into the output may actually be very small, because the ripple voltage seen at the injection point may be quite small. An ideal injector would thus only inject an ac current into the output while only overcoming a small ac voltage ripple to do so, thus achieving low dissipation.

To date, the injection method most closely approaching this ideal is the use of a linear amplifier which drives the injection current onto the output through a current transformer and coupling capacitor [3,6]. The current transformer converts the relatively high-voltage low-current output of the linear amplifier to a low-voltage, high-current injection signal, while the capacitor ac-couples the signal to the injection point. Injection levels of as much as an amp have been achieved without undue dissipation using this method [6]. The drawbacks to this approach are the cost and volume of the current transformer and coupling capacitor, and the performance limitations introduced by their parasitics.

An alternative to this approach is the use of a class A stage to inject current onto the output. While far less efficient than the former method, this approach has the advantage of extreme simplicity, and accurate, high-bandwidth current injection is easily achieved [7,9]. Furthermore, when the dc voltage at the injection point is low, the injector can be directly coupled to the filter output without undue losses. For example, in the prototype system developed here, a 125 mA bias current drawn directly from the 14 V injection node causes only 1.75 W of dissipation, which is less than 1% of converter output power. Because of the simplicity of this approach, we have implemented a class A output injector in the prototype active filter. Figure 4 shows the direct-coupled class-A injector circuit we have employed. An LM6361 op amp is used along with a ZTX 649 transistor in our implementation. Additional circuitry (not shown) is used for protection and current limiting in the injector circuit.

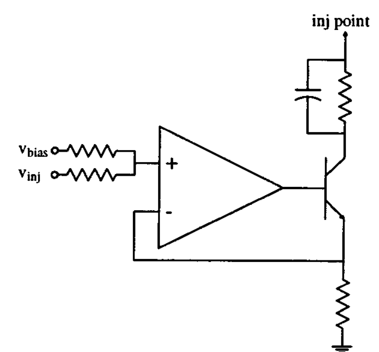

Figure 4 The class A current injection circuit.

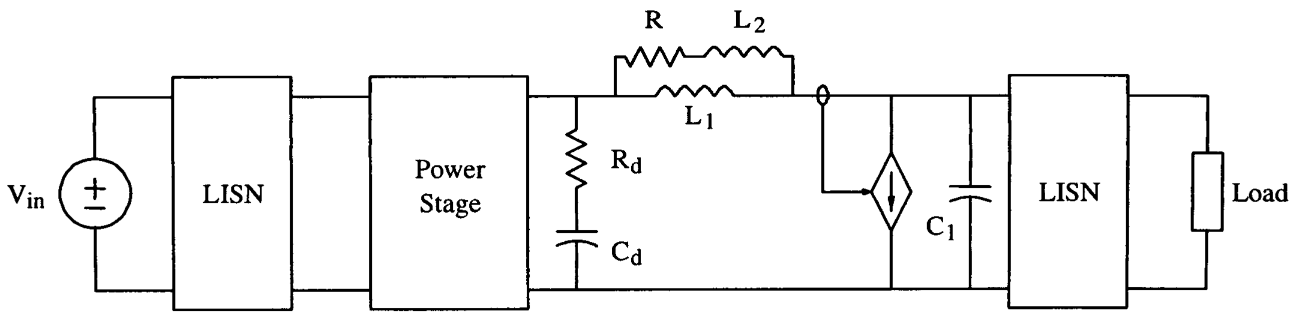

Figure 5 The experimental setup used to test the new active filtering method.

III. Prototype Converter System

The proposed active filter technique has been applied to the output filter of a 230 W, 125 kHz buck converter with a 42 V nominal input voltage and a 14 V nominal output voltage (Fig. 1). The discontinuous-mode converter uses a 1.4 µH buck inductor and a 20 µF primary output capacitor. The converter operates under averaged current-mode control, and regulates the voltage at the inside of the EMI filter so that the filter dynamics do not appear inside the converter's voltage control loop. A more detailed view of the output filter elements can be found in Fig. 5, which shows the experimental setup used to test the new approach. The passive filter element values used in the hybrid passive/active filter are L_1 = 9 µH, C_1 = 5 µF, L_2 = 51 µH, R = 0.56 Ω, C_d = 47 µF, R_d = 3.3 Ω. The size of the filter inductors L_1 and L_2 are such that they carry a total of approximately 100 mA of ripple current. The active filter is designed to cancel this ripple current.

It should be pointed out that despite the term "feedforward" active filter, the active element *does* affect the dynamics of the hybrid passive/active filter. This is because the current being canceled is not an independent input, but is in fact a function of the output voltage, which is in turn affected by the injected current. Nevertheless, starting with a transfer function from sensed to injected current, the dynamics of the hybrid filter system are easily determined. In the case studied here, the addition of the active element reduces the filter damping; the introduction of the small RC damping leg in the filter was in response to this effect.

IV. Experimental Results

Tests of the active filter circuit were conducted with the experimental setup shown in Fig. 5, using conventional EMI test methods. Experiments were carried out over a ground plane, and 50 Ω Line Impedance Stabilization Networks (LISNs) were employed to provide controlled ripple-frequency impedances at the input and output of the system under test. (A LISN is a filter which passes power-frequency currents, but which shunts ripple frequency currents into a known impedance.) The LISN ripple voltage (the standard metric in conducted EMI specifications) was used to evaluate filter effectiveness; this is equivalent to measuring the current into the 50 Ω ripple-frequency impedance of the LISN. Except as noted, all experimental results have been obtained with a 1 Ω resistive load. The following test procedure was used: First, measurements were made using only the passive portion of the hybrid passive/active filter. Next, the active filter portion was added in, and a second set of measurements was taken. Finally, an entirely passive filter was designed which allows the converter to meet the same ripple specification as with the hybrid passive/active filter, and a final set of measurements was taken using this entirely passive filter.

A. Hybrid Passive/Active Filter

Figure 6a shows the LISN voltage using only the passive portion of the hybrid filter, while Fig. 6b shows the LISN voltage with the active element of the hybrid filter included. There is clearly a substantial reduction in the switching ripple when the active filter element is employed. Figure 7 shows the spectrum of the LISN voltage both with and without the use of the active filter element. A reduction of over 30 dB is achieved in the fundamental ripple component through use of the active filter. Note that significant reductions are not achieved at higher frequencies. This is not because the active filter does not have enough bandwidth; rather, these components are so small that they are at the noise and pickup floor of the prototype active filter, and hence cannot be effectively eliminated by it. Nevertheless, through use of the active filter element, the converter is able to meet a ripple specification that is flat across frequency (63 dB µV), which it would not meet using only the passive portion of the filter.

B. Comparison to an Equivalent Passive Filter

In order to provide a fair assessment of the advantages of the proposed active filter method, an entirely passive filter was designed which allows the converter to meet the same flat ripple specification across frequency as with the hybrid filter. The passive filter was constructed using the same filter topology as the passive portion of the hybrid filter. Referring to Fig. 5, the component values for the entirely passive filter were selected as: L_1 = 225 µH, C_1 = 5 µF, L_2 = 576 µH, R = 1.9 Ω, C_d = 47 µF, R_d = 3.3 Ω.

Figure 8 shows the spectrum of the LISN voltage for both

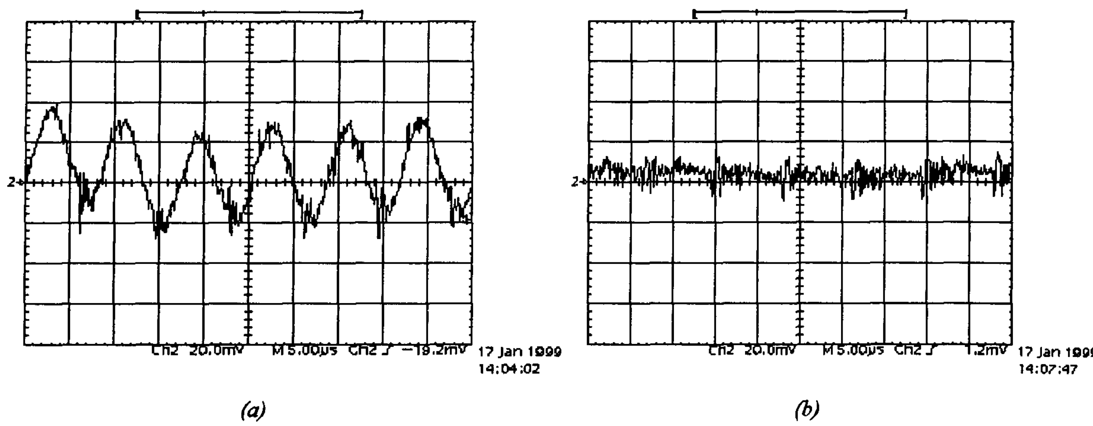

Figure 6 LISN output voltage for converter with hybrid passive/active output filter operating at 1Ω load. (a) Only the passive portion of the hybrid filter (without active cancellation). (b) Full hybrid filter (with active cancellation).

the hybrid filter and the entirely passive filter. Each filter allows the converter to meet the same flat ripple specification (63 dB μV). At higher frequencies, the entirely passive filter provides more attenuation than the hybrid filter. This is essentially because it had to be overdesigned for high frequencies in order to meet the ripple specification at the fundamental (which is the hardest component to attenuate with a passive filter). The important result, however, is the relative size of the two filters. The weight of the hybrid filter is only 20% of that of the passive filter! Thus, through use of the active filtering technique a factor of 5 reduction in overall filter mass has been achieved.

A second advantage of the active filtering approach is in the transient performance of the system. Because a hybrid passive/active filter can employ smaller passive (energy storage) components than an entirely passive filter, it is expected that one can achieve faster dynamic control of the output when active filtering techniques are used. (Note that because the active filtering circuitry can only inject small-signal currents, it has very little effect during large-signal transients.) To investigate this, the output voltage response to load transients was measured both with the hybrid filter and with the entirely passive filter. (The LISNs were not employed during these tests, as only the low-frequency transient response was of interest.) Figure 9a shows the output voltage response of the system to a load step from 3 Ω to 1.5 Ω using the entirely passive filter, while Fig. 9b shows the response to the same load step using the hybrid filter. Both the magnitude and

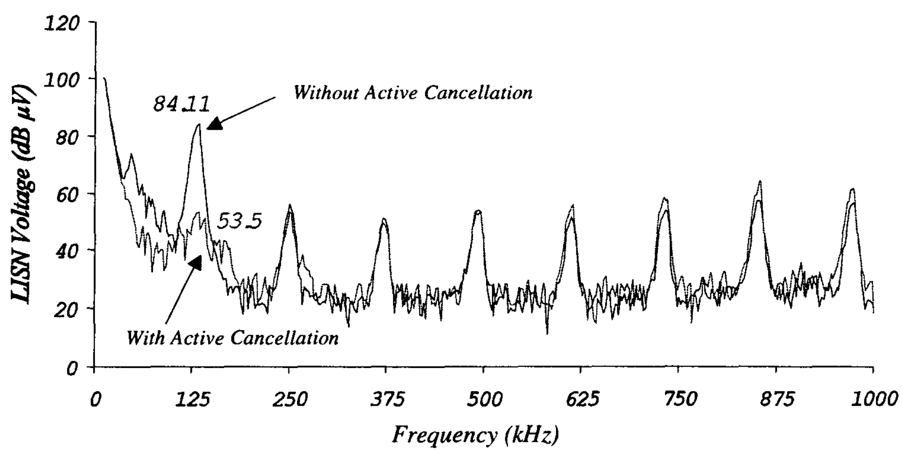

Figure 7 LISN output voltage spectra for converter operation with the hybrid passive/active filter. Plots are shown for operation both with and without active cancellation. Use of active cancellation results in more than a 30 dB reduction in the fundamental ripple voltage.

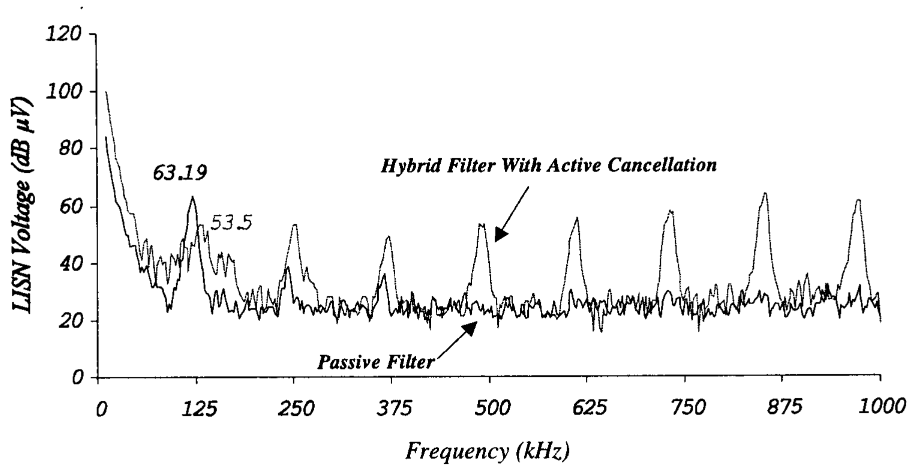

Figure 8 LISN output voltage spectra for converter operation with two different filters. Plots are shown for operation with the hybrid passive/active filter, and also with an entirely passive filter. The two filters meet the same flat ripple specification (~ 63 dBμV), but the hybrid filter is substantially smaller.

duration of the output voltage transient are substantially smaller when the hybrid filter is used, demonstrating the advantages in transient performance that can be obtained using the active filtering approach.

V. CONCLUSIONS

This paper presents the design and evaluation of a feedforward ripple-current active filter which employs a Rogowski-coil current sensor. A coil and amplifier design suited to the application is developed, allowing a number of advantages of the approach to be realized, including high accuracy and bandwidth, low weight and cost, and low sensitivity to parameter variations. The design of current injectors for feedforward active filters is also considered, and an appropriate injection circuit is implemented. The active ripple filter is employed in the design of an output filter for a 230 W dc/dc converter.

Experimental results demonstrate the feasibility of the new active filter, and illustrate its potential benefits. It has been shown that the approach provides substantial reductions in power converter ripple, thus allowing considerable reductions in the size of passive filter elements. In the example investigated here, a factor of five reduction in total filter mass was achieved using the approach. Furthermore, it has been demonstrated that the approach allows substantial improvement in the dynamic control of the converter output due to the reduction in passive filter size.

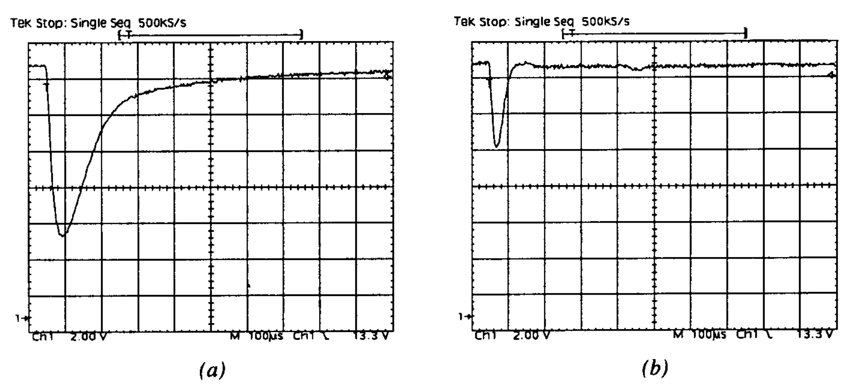

Figure 9 Output voltage transient response of the converter for a load step from 3 Ω to 1.5 Ω. (a) Response using entirely passive filter. (b) Response with hybrid passive/active filter. The transient magnitude and duration are far smaller with the hybrid filter.

ACKNOWLEDGMENTS

The authors would like to acknowledge the support for this research provided by the United States Office of Naval Research under grant number N00014-96-1-0524, and by the member companies of the MIT/Industry Consortium on Advanced Automotive Electrical/Electronic Components and Systems.

REFERENCES

[1] T.K. Phelps and W.S. Tate, "Optimizing Passive Input Filter Design," *Proceedings of Powercon 6*, May 1979, pp. G1-1 - G1-10.

[2] M.J. Nave, Power Line Filter Design for Switched-Mode Power Supplies, New York: Van Nostrand Reinhold, 1991.

[3] J. Walker, "Design of Practical and Effective Active EMI filters," *Proceedings of Poweron 11*, 1984, I-3 pp. 1-8.

[4] L.E. LaWhite and M.F. Schlecht, "Active Filters for 1-MHz Power Circuits with Strict Input/Output Ripple Requirements," *IEEE Trans. Power Electron.*, Vol. PE-2, No. 4, Oct. 1987, pp. 282-290.

[5] T. Farkas and M.F. Schlecht, "Viability of Active EMI Filters for Utility Applications," *IEEE Trans. Power Electron.*, Vol. 9, No. 3, May 1994, pp. 328-337.

[6] P. Midya and P.T. Krein, "Feed-forward Active Filter for Output Ripple Cancellation," *Int. J. Elec.*, Vol. 77, No. 5, pp. 805-818.

[7] D.C. Hamill, "An Efficient Active Ripple Filter for Use in DC-DC Conversion," *IEEE Trans. Aero. and Electron. Sys.*, Vol. 32, No. 3, July 1996, pp. 1077-1084.

[8] M.S. Moon and B.H. Cho, "Novel Active Ripple Filter for the Solar Array Shunt Switching Unit," *J. Propulsion and Power*, Vol. 12, No. 1, Jan/Feb 1996, pp. 78-82.

[9] M.T. Thompson and M.F. Schlecht, "High Power Laser Diode Driver Based on Power Converter Technology," *IEEE Trans. Power Electron.*, Vol. 12, No. 1, Jan 1997, pp. 46-52.

[10] W. Rogowski and W. Steinhaus, "Die Messung der Magnetischen Spannung," *Arch. Electrotech.* 1, 1912.

[11] W.F. Ray and R.M. Davis, "Wide Bandwidth Rogowski Current Transducers, Part 1: The Rogowski Coil," *EPE Journal*, Vol. 3, No. 1, March 1993, pp. 51-59.

[12] A. Radun, "An Alternative Low-Cost Current-Sensing Scheme for High-Current Power Electronics Circuits," *IEEE Trans. Industrial Elec.*, Vol. 42, No. 1, Feb. 1995, pp. 78-84.